



High-intensity, long-duration, continuous AE activity events associated with Alfvénic fluctuations in 2003

Alan Prestes, Virginia Klausner, and Arian Ojeda-González

Vale do Paraíba University – UNIVAP 12244-000, São José dos Campos, SP, Brazil

Correspondence to: Virginia Klausner (viklausner@gmail.com)

Received: 19 June 2017 – Revised: 25 September 2017 – Accepted: 2 October 2017 – Published: 13 November 2017

Abstract. The interaction between a fast-speed and a low-speed stream causes large-amplitude Alfvénic fluctuations; consequently, the intermittency and the brief intervals of southward magnetic field associated with Alfvén waves may cause high levels of AE activity, the so-called high-intensity, long-duration, continuous AE activity (HILDCAA). In this article, the 4 h windowed Pearson cross-correlation (4WPCC) between the solar wind velocity and the interplanetary magnetic field (IMF) components is performed in order to confirm that the less strict HILDCAA (HILDCAAs*) events include a larger number of Alfvén waves than the HILDCAA events, once HILDCAAs disregard part of the phenomenon. Actually, a HILDCAA event is entirely contained within a HILDCAA* event. However, the opposite is not necessarily true. This article provides a new insight, since the increase of Alfvén waves results in an increase of auroral electrojet activity; consequently, it can cause HILDCAAs* events. Another important aspect of this article is that the superposed epoch analysis (SEA) results reaffirm that the HILDCAAs* are associated with high-speed solar streams (HSSs), and also the HILDCAAs* present the same physical characteristics of the traditional HILDCAA events.

Keywords. Magnetospheric physics (solar wind–magnetosphere interactions; storms and substorms; general or miscellaneous)

1 Introduction

During the declining phase of solar cycles, the dominant solar phenomena affecting the geomagnetic activity are coronal holes (Krieger et al., 1973; Hapgood, 1993; Webb, 1995; Tsurutani et al., 2006), which are characterized by excep-

tionally low densities and unipolar photospheric magnetic fields with “open” magnetic field topologies. Some coronal holes can persist over several solar rotations. From coronal holes, high-speed solar streams (HSSs) are continuously emanating, and they can interact with the slower solar-wind streams forming stream-interaction regions. Also, these stream-interaction regions can produce corotating interaction regions (CIRs, Smith and Wolfe, 1976; Gosling and Pizzo, 1999; Heber et al., 1999).

The coronal hole wind is characterized by large-amplitude Alfvén wave trains (Alfvén, 1942; Zirker, 1977; Ofman and Davila, 1995; Tsurutani et al., 1995, 2006; Tsurutani and Ho, 1999). In Alfvén waves within HSSs, the negative interplanetary magnetic field (IMF) B_z component fluctuations induce continuous auroral zone activity, the so-called high-intensity long-duration continuous AE activity (HILDCAA, Tsurutani and González, 1987; Tsurutani et al., 2004; Guarnieri, 2013; Hajra et al., 2013, 2014a; Souza et al., 2016; Prestes et al., 2017). The yearly AE index average can be higher in the solar descending phase and minimum activity due to HSS/CIR events (HSS + CIR and their combination), than during the solar maximum activity, when the geomagnetic activity is usually caused by fast interplanetary coronal mass ejections (ICMEs; Tsurutani and González, 1987; Tsurutani and Ho, 1999; Tsurutani et al., 1995, 2006; Guarnieri, 2013; Ojeda-González et al., 2017b). In solar descending phase and minimum activity, the geomagnetic storms are typically only weak to moderate, and their long recovery phases are due to the highly oscillatory nature of the magnetic field within the CIRs (Tsurutani et al., 2006).

The traditional HILDCAA events are defined by four criteria:

- high-intensity – peak AE values should exceed 1000 nT;

- long-duration – their duration should be longer than 2 days;
- continuous AE activity – the AE values should never drop below 200 nT for more than 2 h at a time;
- HILDCAAs must occur outside of the main phase of geomagnetic storms (Tsurutani et al., 1995, 2004).

Moreover, Prestes et al. (2017) included a small modification in the following criterion: “the AE values should never drop below 200 nT for more than 2 h at a time”, by changing 2 to 4 h at a time, in order to increase the number of HILDCAA events available for study. They defined these slightly modified events as HILDCAAs* (see Prestes et al., 2017, for more details).

The article aims to verify the Alfvénic fluctuations present in the solar wind during HILDCAA and HILDCAA* occurrences. For this reason, we will correlate the solar wind velocity components with their respective IMF components using spectral analysis, in particular, the gapped wavelet transform (GWT). Multi-scaled spectral analysis of the solar parameters and/or the geomagnetic indices and their correlation have been used by many authors (Echer et al., 2004; Prestes et al., 2006; Klausner et al., 2013, 2014, 2016a, b; Ojeda-González et al., 2014, 2017a). If the variations in the solar wind velocity and the IMF are well-correlated, it can be said that there are Alfvénic fluctuations presented in the HSS. Therefore, we expect that these correlations will be higher during HILDCAA and HILDCAA* events, since Alfvén waves usually induce continuous auroral zone activity.

2 Datasets and methodology

In this work, we used the 12 HILDCAA and 26 HILDCAA* events in 2003 previously identified by Prestes et al. (2017). In addition to determine the typical values of the solar wind parameters related to them, we used the measurements by the Advanced Composition Explorer (ACE) satellite with 1 h and 1 min resolutions (Smith et al., 1998; McComas et al., 1998). The interplanetary solar wind data used here are solar wind speed (V_{sw} in km s^{-1}), plasma density (N_{sw} in cm^{-3}), temperature (T_{sw} in K), flow pressure (P_{sw} in nPa), IMF magnitude (B_o in nT) and the B_x (nT), B_y (nT) and B_z (nT) components in the GSM coordinate system. Here, we also used the AE and Dst geomagnetic indices.

In order to show the HSS/CIR occurrence in 2003, a spectral analysis using GWT is performed. The GWT can be used in the analysis of non-stationary signal to obtain information on the frequency or scale variations, and to detect its singularities in time and/or in space (see Klausner et al., 2013, for more details). It is possible to analyze a signal in a timescale plane, known as wavelet scalogram. In analogy with the Fourier analysis, the square modulus of the wavelet

coefficient $|W(a, b)|^2$ is used to provide the energy distribution in the timescale plane. In the GWT analysis, we can also explore the central frequencies of the time series through the global wavelet spectrum, which is the spectral power at each scale integrated over the whole time series. Moreover, the GWT is used to reduce gap problems in data, considering that it restores the admissibility condition, when the wavelet is broken due to the overlap of the data gaps (Klausner et al., 2013). On the one hand, the continuous wavelet transform (CWT) of a function $f(t)$ is defined by the integral transform, $W(a, b) = \int f(t) \frac{1}{\sqrt{a}} \psi^* \left(\frac{t-b}{a} \right) dt$, where ψ is the wavelet mother that is a function of both time and frequency (time b and scale a), and $*$ represents the complex conjugate. On the other hand, in the GWT near a gap, the wavelet mother function $\psi'_{a,b}(t) = \frac{1}{\sqrt{a}} \psi \left(\frac{t-b}{a} \right) G(t)$ is used instead of ψ , where $G(t)$ is the function of data gaps. The leading idea of the GWT is to restore the admissibility condition by repairing in some way the wavelet itself (see Klausner et al., 2013, for more details). Therefore, the GWT will be used here to help reduce the effects of two common problems of the spectral analysis: (i) the presence of gaps in time series and (ii) boundary effects due to their finite length.

For the purpose of associating the HILDCAA* events with HSS/CIR events, superposed epoch analysis (SEA) is applied to the solar wind parameters (V_{sw} , N_{sw} , T_{sw} , P_{sw} , IMF B_o , B_x , B_y and B_z) and to the geomagnetic indices (Dst and AE), during the HILDCAA* events in 2003. As discussed by Prestes et al. (2017), the HILDCAA event as defined by Tsurutani and González (1987) is entirely contained within a HILDCAA* event. For this reason, in each IMF parameter and in each geomagnetic index, we choose 2 days prior and 2 days after of the HILDCAA*/HILDCAA onset using 1 h time resolution. The length of 2 days is chosen because it is one of the four criteria for an event to be considered HILDCAAs*/HILDCAAs. Following the same methodology applied by Hajra et al. (2013, 2014b), we consider the initiation time of HILDCAA*/HILDCAA events as the zero epoch time. Further, we calculate the mean variation of each IMF parameter and each geomagnetic index for the 2 days prior and for the 2 days after of the zero epoch time.

Until this point, the possibility of HILDCAA*/HILDCAA events associated with Alfvén waves remains an unsolved issue. To solve this problem, we implement a 4 h windowed Pearson cross-correlation (4WPCC) methodology, which is a well-accepted methodology by the scientific community to identify Alfvén waves in the solar wind intervals. As an example, this methodology was used in Belcher et al. (1969) and Tsurutani et al. (1990, 2011) to determine the Alfvénicity or non-Alfvénicity of the interplanetary medium. In these works, the 4WPCC of the individual vector components of the magnetic field and the solar wind velocity at 0 h lag were calculated.

Therefore, the 4WPCC between the IMF components and the solar wind velocity components ($V_x - B_x$, $V_y - B_y$, and

$V_z - B_z$) at 0 h lag are calculated in the same way as done by Tsurutani et al. (2011). And it is applied to the ACE satellite dataset (see in ACE Level 2 data server: merged IMF and solar wind 64 s averages). The Alfvénicity behavior is analyzed throughout the year of 2003. Following, the results will be presented.

3 Results and discussion

In this section, we will study the AE activity index variation and the HILDCAA*/HILDCAA Alfvénicity behavior. But first we will present the multi-scaled spectral analysis of solar and/or geomagnetic activity to determine which of the dynamical geomagnetic storm processes are responsible for energy deposition into the magnetosphere. In this case, it is expected that HSSs/CIRs are responsible for the recurrent low-to-moderate geomagnetic activity in 2003 and for the energy deposition in the auroral zone. Second, we will evaluate that the occurrence of HILDCAAs* is associated with HSS/CIR events as discussed by Prestes et al. (2017). Therefore, the SEA will be applied to the geomagnetic and solar/interplanetary data.

Figure 1 presents the time series (top left panel) of (a) plasma density (N_{sw} in cm^{-3}), (b) Dst (nT), (c) AE (nT), (d) solar wind speed (V_{sw} in km s^{-1}), (e) B_z (nT) component of IMF (GSM coordinates) and (f) IMF magnitude (B_o in nT); their respective wavelet square modulus (bottom left panel); and their respective global wavelet spectrum (total energy in each scale – bottom right panel).

In the top panel, Fig. 1 gives the daily average of the IMF and plasma data for the year 2003. This figure also shows an overview of the geomagnetic activity for this entire year. When the lowest daily average of the solar wind proton density occurs simultaneously with the highest average of solar wind speed, it indicates the presence of HSSs (Jian et al., 2006).

In the bottom panel of Fig. 1, areas of stronger wavelet power are shown in dark red and the areas of lower wavelet power are shown in dark blue. On the x axis, the time variation is plotted with a 10-day interval, and the scale variation with an interval of days is plotted on the y axis. As discussed by Klausner et al. (2016b) using wavelet techniques, the periodicities of 5, 7 and 27 days, and the sub-harmonics of Sun rotation of 9 and 13.5 days present in the scalograms can be associated with HSSs and CIRs (Gosling et al., 1976, 1977). It can be noticed that these periodicities are also presented in the wavelet scalograms of the interplanetary parameters and of the geomagnetic indices in Fig. 1. As well, these scalograms show these similar spectral features in time and scale. Consequently, it is possible to say that the majority of geomagnetic events in 2003 may be associated with HSS/CIR events.

By the way, the HILDCAA*/HILDCAA occurrence also depends on the southward IMF (B_z) fluctuations. The cou-

pling solar-wind–magnetosphere is most strongly controlled by the direction of the IMF, and it is stronger when the IMF is southward. Due to the association of HILDCAAs*/HILDCAAs with HSS/CIR events, it is expected to be a highly oscillatory nature of the B_z . Figure 2 shows the wavelet coherency scalogram between B_z component and the hourly AE index in 2003. The wavelet coherency transform returns the magnitude-squared wavelet coherence, which is a measure of the correlation between signals B_z and AE in the time–frequency plane. In Fig. 2, the strongest levels of energy appear between 13 and 30 days, which are the harmonic and sub-harmonic of the solar rotation. In addition, the periodicity of ~ 27 days persists mostly throughout the year of 2003. This result confirms that the B_z is mainly controlled by HSSs during this year. Therefore, this fact imposes a significantly contribution for HILDCAA*/HILDCAA occurrences.

Moreover, a total of 26 HILDCAA* events (12 HILDCAA events within these HILDCAA* events) have been found in 2003, ~ 2.5 events per month (see Tables 1 and 2 in Prestes et al., 2017). With this result in hand, we decided to verify the solar wind behavior during 2003. Figure 3 shows the daily time series of solar wind speed (black line), and the same signal filtered using a Butterworth low-pass filter with a cutoff frequency (f_c) of 826.72 nHz (red line), which highlights periods above half solar rotation. In other words, the low-pass filter is used to remove all low-order periods up to 14 days from the inputted solar wind series. These periods can be eliminated from the analysis of HSS without compromising the results, and/or even considered background noise. The numbers 1 and 2 indicate the sequence of HSSs, and the presence of two events per solar rotation in mostly months in 2003 can be observed. However, a few months present many HSSs, sometimes more than two per solar rotation. August 2003 is an example of a month with the presence of many HSSs. Also, some streams have profiles which indicate that they are composed of overlapping events, whereas others only have one event. These facts may explain the large number of HILDCAA*/HILDCAA occurrences per month in 2003 found by Prestes et al. (2017).

From this point forward, we will demonstrate that HILDCAA* events are associated with HSS/CIR events. Figure 4 shows the superposed mean variations (solid curves) and the standard deviations (vertical bars) of V_{sw} , N_{sw} , T_{sw} , P_{sw} , IMF B_o , B_x , B_y , B_z , Dst and AE indices. Each panel presents a horizontal line that can be used as a reference parameter. These lines correspond to the 2003 annual mean variation of V_{sw} , N_{sw} , T_{sw} , P_{sw} , IMF B_o and AE, and to the zero value in the case of B_x , B_y , B_z and Dst (see Prestes et al., 2006, for more details). As discussed by Hajra et al. (2013, 2014b), the SEA of the IMF parameters and the SEA of the geomagnetic indices show typical interplanetary signatures of CIRs. An increase of V_{sw} and T_{sw} after the zero epoch time is observed, which represents the compressed fast stream arrival. Also, the interaction between the HSS and the slow-speed stream is evident due to the increase of V_{sw} around the zero epoch

Table 1. HILDCAA events for the year 2003. The HILDCAA events with 4WPCC higher than the 4WPCC annual average are highlighted in bold.

H	$V_x - B_x$ (%)	$V_y - B_y$ (%)	$V_z - B_z$ (%)	Non-H	$V_x - B_x$ (%)	$V_y - B_y$ (%)	$V_z - B_z$ (%)
01	88.0	87.5	91.8	00–01	72.3	76.1	79.2
02	79.7	87.9	86.0	01–02	79.1	81.9	83.6
03	78.6	85.8	91.5	02–03	72.1	78.8	77.5
04	86.8	93.3	94.2	03–04	–	–	–
05	87.7	84.5	91.3	04–05	62.5	65.0	70.6
06	80.9	85.1	90.9	05–06	81.3	91.8	91.8
07	84.8	90.3	90.4	06–07	71.9	77.4	75.5
08	82.2	83.8	81.8	07–08	73.6	77.7	76.9
09	72.9	86.8	85.3	08–09	81.4	83.8	89.3
10	88.3	92.3	93.1	09–10	64.3	71.6	70.3
11	77.5	89.3	90.6	10–11	68.9	72.5	73.7
12	85.5	91.9	93.1	11–12	70.5	78.9	79.4
–	–	–	–	12–13	68.4	75.2	75.8
$\langle \text{Avg.} \rangle :$				$\langle \text{Avg.} \rangle :$	72.2	77.6	78.6
Alfv. (%)				Alfv. (%)	33.3	50.0	41.6

Table 2. HILDCAA* events for the year 2003. The HILDCAA* events with 4WPCC higher than the 4WPCC annual average are highlighted in bold.

H*	$V_x - B_x$ (%)	$V_y - B_y$ (%)	$V_z - B_z$ (%)	Non-H*	$V_x - B_x$ (%)	$V_y - B_y$ (%)	$V_z - B_z$ (%)
01	72.8	78.2	84.6	00–01	69.9	73.0	73.8
02	77.9	87.5	85.4	02–03	83.9	84.0	76.3
03	89.9	92.0	90.7	03–04	65.0	66.3	75.0
04	75.2	81.9	82.3	04–05	75.8	75.6	85.7
05	88.6	87.9	91.6	05–06	69.2	77.7	80.7
06	87.4	85.6	91.4	06–07	85.1	84.2	86.5
07	81.0	90.8	93.4	07–08	76.0	79.2	81.0
08	75.8	77.1	77.1	08–09	84.3	90.9	90.1
09	79.7	87.9	86.0	09–10	80.6	80.2	91.6
10	68.8	75.7	76.3	10–11	73.5	80.2	77.2
11	83.9	81.2	86.7	11–12	75.2	69.5	72.4
12	82.7	89.4	92.8	12–13	59.4	59.5	55.8
13	84.2	86.8	91.4	13–14	63.6	68.4	70.5
14	82.2	88.6	90.5	14–15	59.7	66.8	62.2
15	61.3	66.5	60.8	15–16	44.6	70.0	62.7
16	78.0	84.2	83.3	16–17	76.9	79.6	81.6
17	68.3	71.9	73.9	17–18	57.0	57.9	63.4
18	81.3	90.2	93.4	18–19	68.8	77.7	76.4
19	84.9	91.9	89.5	19–20	68.0	64.5	69.9
20	85.1	88.4	92.1	20–21	66.3	64.1	58.3
21	85.1	87.9	94.1	21–22	69.9	71.5	68.3
22	86.2	93.1	92.5	22–23	71.0	77.4	78.0
23	81.4	92.3	88.7	23–24	59.1	67.0	68.1
24	62.3	70.5	72.3	24–25	64.7	67.7	70.0
25	77.5	89.3	90.6	25–26	66.7	68.3	77.0
26	84.0	90.5	91.9	26–27	70.5	78.9	79.4
27	–	–	–	27–28	68.3	74.3	77.4
$\langle \text{Avg.} \rangle :$				$\langle \text{Avg.} \rangle :$	69.4	73.1	74.4
Alfv. (%)				Alfv. (%)	33.3	40.7	29.6

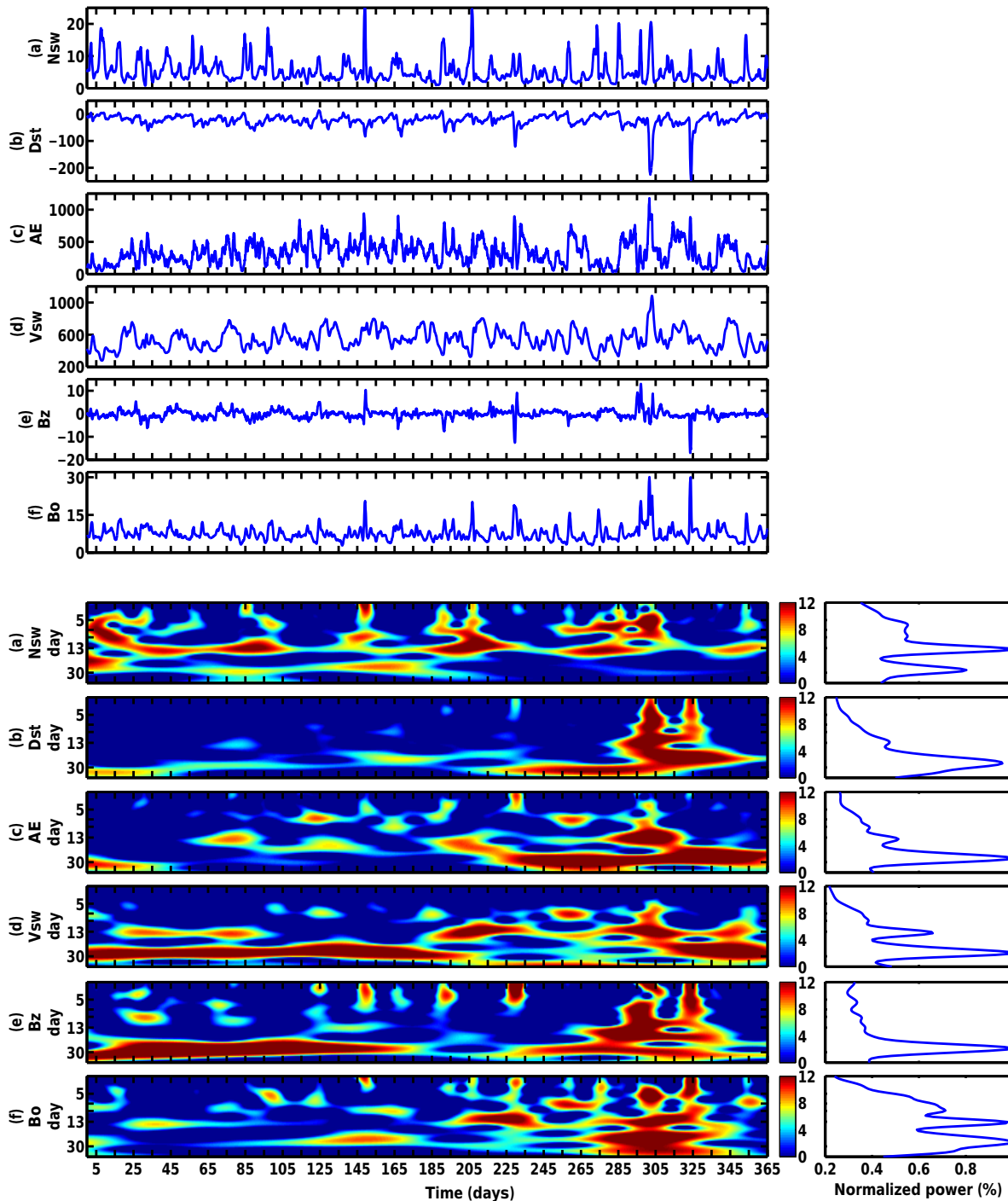


Figure 1. From top to bottom, the upper panel shows the time series and the bottom panel shows wavelet scalogram and global normalized wavelet spectrum of (a) plasma density (N_{sw} in cm^{-3}), (b) Dst (nT), (c) AE (nT), (d) solar wind speed (V_{sw} in km s^{-1}), (e) B_z (nT) component of IMF (GSM coordinates) and (f) IMF magnitude (B_o in nT).

time. On the other hand, N_{sw} , P_{sw} , B_o and B_z present an increase prior to the zero epoch time, which represents a compression of the slow solar wind leading to higher plasma densities, pressure and magnetic fields. However, the increase of N_{sw} , P_{sw} , B_o and B_z prior to the zero epoch occur at differ-

ent time lags, and also, in all these parameters, their increases are in the points of largest standard deviation. This fact may be explained by some HILDCAA*/HILDCAA events associated with weak ring current enhancements ($\text{Dst} \geq -50$ nT) and/or with recovery phases of geomagnetic storms. Similar

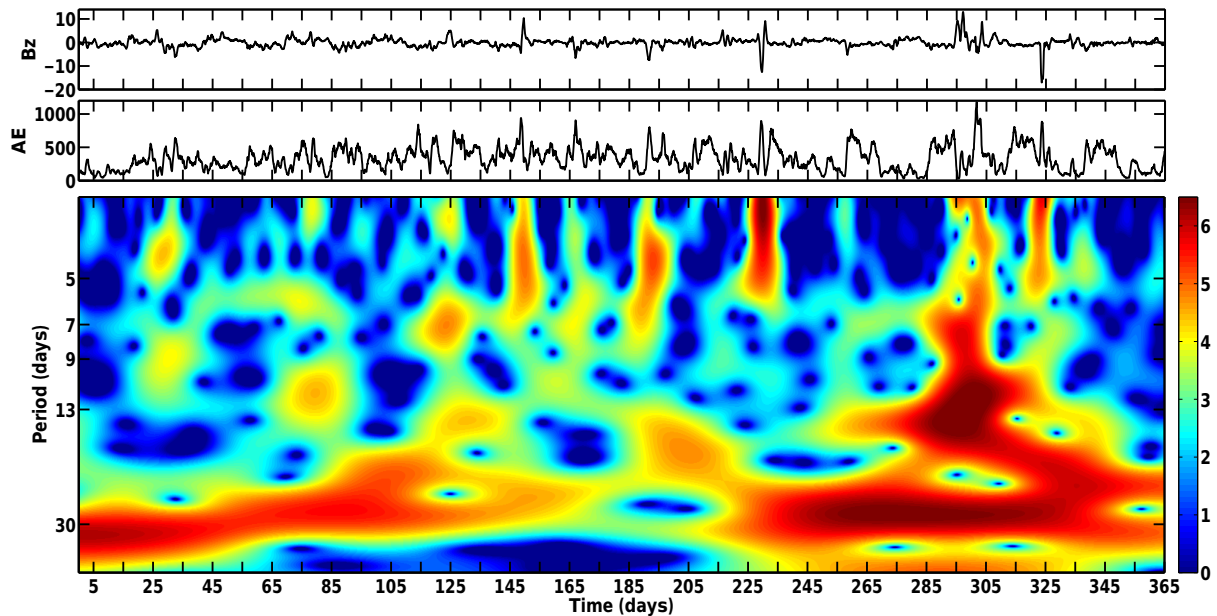


Figure 2. Morlet wavelet coherency scalogram between B_z component of IMF and the AE hourly index.

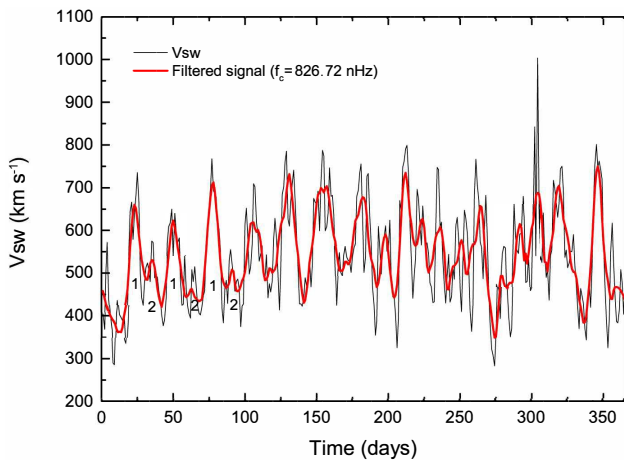


Figure 3. Daily time series of solar wind speed for 2003 (black line) and low-pass filter with a cutoff frequency (f_c) of 826.72 nHz (red line).

features were observed by Hajra et al. (2013, 2014b) in the analysis of HILDCAA events using SEA.

From this point forward, the possibility of HILDCAA/HILDCAA* association with the Alfvén waves will be discussed. Figure 5 shows the 4WPCC between the solar wind velocity z component and the IMF z component ($V_z - B_z$) versus time for the whole year, at 0 h lag. The 4WPCC annual mean $V_z - B_z$ is 79 %, while for the 4WPCC between the solar wind velocity x component and the IMF x component ($V_x - B_x$), and between the solar wind velocity y component and the IMF y component ($V_y - B_y$) they are 73 and 77 %, respectively. The year of 2003 has shown the

highest 4WPCC annual mean in the solar cycle 23. This fact means that there are a great number of Alfvén waves during this year and, consequently, an enhancement of the number of HILDCAA events as observed by Hajra et al. (2013) and Prestes et al. (2017).

For each HILDCAA event, the 4WPCC is calculated, and these results are shown in the first four columns of Table 1. The HILDCAA events with 4WPCC higher than the 4WPCC annual average are highlighted in bold. Only one HILDCAA event has the cross-correlation lower than the annual average. This result represents that 97.2 % of the total number of events have the 4WPCC higher than the annual average, as show in the last line of Table 1. The same analysis is performed in the periods of non-HILDCAA events, and the results are shown in the last four columns of Table 1. The number of intervals with 4WPCC higher than 4WPCC annual average is ~ 42 %. This percentage is very high considering that it corresponds to non-HILDCAA events.

Afterwards, we applied the same 4WPCC methodology previously used in the HILDCAA events to HILDCAAs*. Therefore, Table 2 is very similar to Table 1 but for the HILDCAA* events. It can be noticed that ~ 84 % of HILDCAA* events have higher 4WPCC values than the average. And the main result is that the number of non-HILDCAA* events presents a decrease of 4WPCC values in about ~ 34 %.

Moreover, a total of six graphics (not all shown here) were plotted, each one of them showing the 4WPCC of $V_x - B_x$, $V_y - B_y$ and $V_z - B_z$ versus number of HILDCAA and/or HILDCAA* events in 2003. Once more, it can be noticed that the HILDCAA*/HILDCAA events

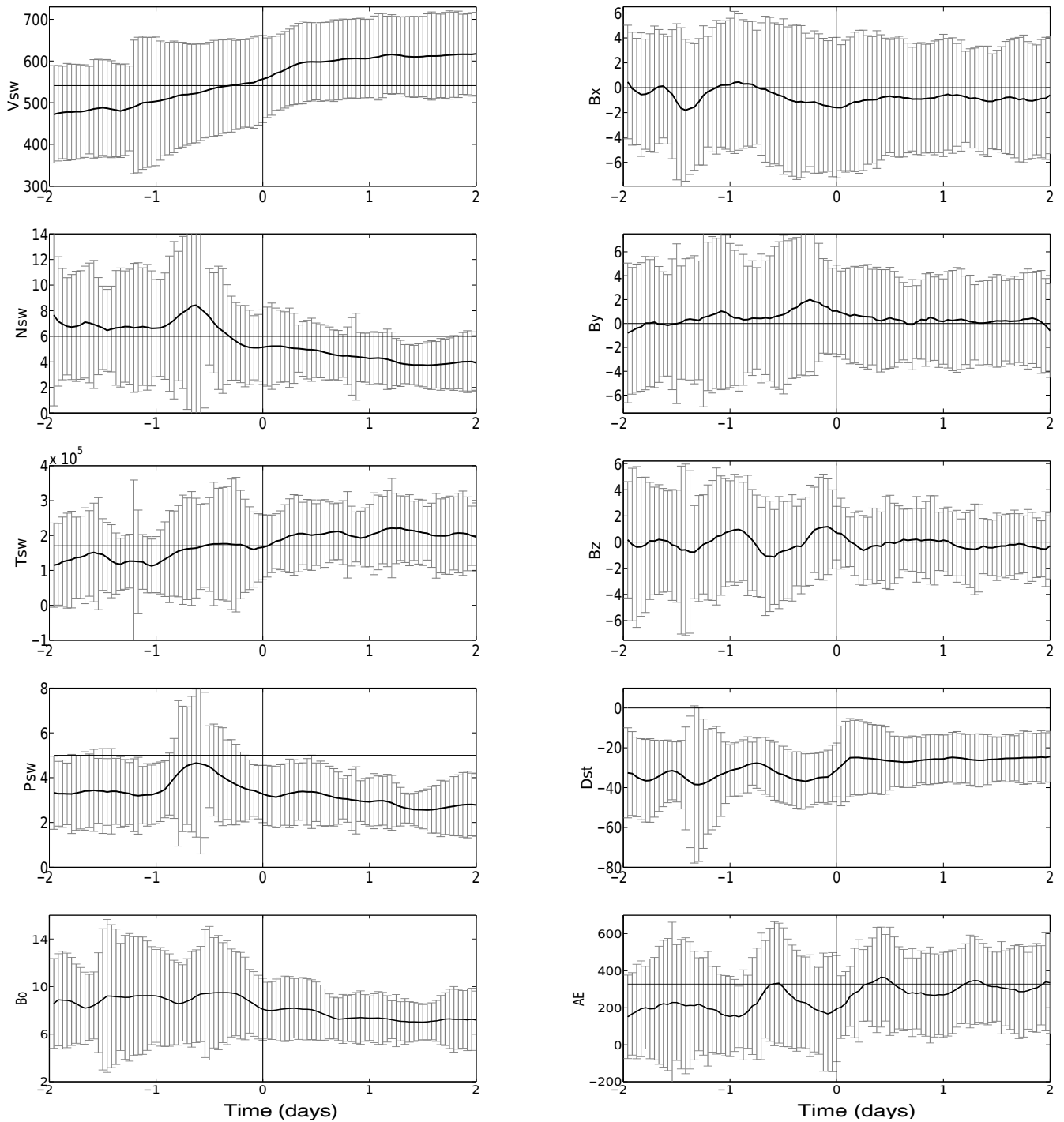


Figure 4. From top to bottom and from left to right, panels show the SEA results of solar wind speed (V_{sw} in km s^{-1}), plasma density (N_{sw} in cm^{-3}), temperature (T_{sw} in K), flow pressure (P_{sw} in nPa), IMF magnitude (B_0 in nT), the B_x (nT), B_y (nT), B_z (nT) components in the GSM coordinate system, and the Dst (nT) and AE (nT) indices, respectively. The curves show the average values while the vertical bars show the standard deviations. On the horizontal axis, the zero epoch time corresponds to the HILDCAAs* onset, and the SEA is performed from 2 days prior to 2 days after the zero epoch time.

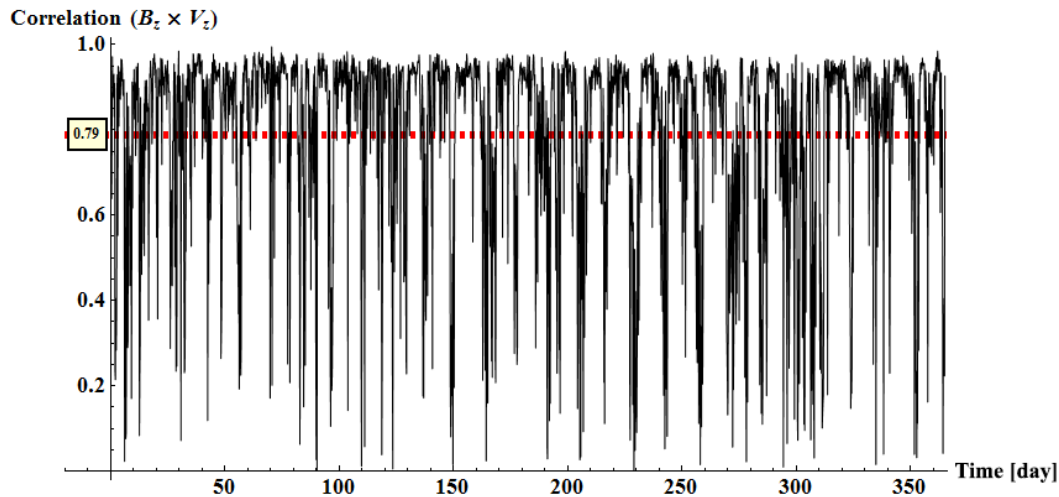


Figure 5. 4 h windowed Pearson cross-correlation between the solar wind velocity z component and the IMF z component ($V_z - B_z$) versus time for the whole year of 2003, at 0 h lag.

present higher correlation values than the periods of non-HILDCAAs*/HILDCAAs. And the decrease of 4WPCC values in periods of non-HILDCAAs* leads us to suggest that the HILDCAA* events include a greater number of Alfvén waves than the HILDCAA events, because HILDCAAs disregard part of the phenomenon.

4 Conclusions

The declining phase of the cycle 23, especially the year of 2003, was exceptional in producing intense and continuous AE geomagnetic activity because there were more than two corotating streams present in each month as observed here. In conclusion, the Earth's magnetosphere was impinged twice by these streams during each ~ 27 -day period, similar to the results found by Tsurutani et al. (1995) in the declining phase of the solar cycle 20 (year of 1974). Consequently, a great number of HILDCAA* events occurred in 2003, and this fact may be explained by solar energy transfer into the magnetosphere by the Alfvén waves. These waves can be generated by HSSs, which mostly originated from coronal holes.

The following results can be highlighted from the present study:

- The SEA results confirm that the HILDCAAs* are associated with HSS/CIR events, and also they present the same physical characteristics of the traditional HILDCAA events as discussed by Prestes et al. (2017).
- The higher 4WPCC values between the solar wind velocity and the IMF component during HILDCAAs* than during HILDCAA reaffirm that these events include a greater number of Alfvén waves, once HILDCAAs disregard part of the phenomenon.

- The high number of HILDCAA* occurrences per month in 2003 may be caused by Alfvén waves.

These results are encouraging, and they suggest that the HILDCAAs* may potentially be used as an alternative way of explaining the Alfvénic effects in the AE index.

Data availability. The dataset used in this paper can be downloaded from WDC-Kyoto and OMNIWeb home pages. The AE and Dst indices were downloaded from the World Data Center for Geomagnetism –Kyoto (<http://wdc.kugi.kyoto-u.ac.jp/index.html>). The ACE parameters are available through the National Space Science Data Center (OMNIWeb): <http://omniweb.gsfc.nasa.gov/form/dx1.html>.

Competing interests. The authors declare that they have no conflict of interest.

Special issue statement. This article is part of the special issue “Space weather connections to near-Earth space and the atmosphere”. It is a result of 6^o Simpósio Brasileiro de Geofísica Espacial e Aeronomia (SBGEA), Jataí, Brazil, 26–30 September 2016.

Acknowledgements. This research was supported by CNPq (no. 301441/2013-8) and FAPESP (no. 2009/02907-8) grants awarded to Alan Prestes. Virginia Klausner wishes to thank CNPq for the financial support for her postdoctoral research (grants 165873/2015-9).

The topical editor, Jean-Pierre Raulin, thanks Sergey Sokolov and Maurício Bolzan for help in evaluating this paper.

References

- Alfvén, H.: Existence of Electromagnetic-Hydrodynamic Waves, *Nature*, 150, 405–406, <https://doi.org/10.1038/150405d0>, 1942.
- Belcher, J. W., Davis, L., and Smith, E. J.: Large-amplitude Alfvén waves in the interplanetary medium: Mariner 5, *J. Geophys. Res.*, 74, 2302–2308, <https://doi.org/10.1029/JA076i016p03534>, 1969.
- Echer, E., González, W., González, A., Prestes, A., Vieira, L., Lago, A. D., Guarnieri, F., and Schuch, N.: Long-term correlation between solar and geomagnetic activity, *J. Atmos. Solar-Terr. Phys.*, 66, 1019–1025, <https://doi.org/10.1016/j.jastp.2004.03.011>, 2004.
- Gosling, J. and Pizzo, V.: Formation and Evolution of Corotating Interaction Regions and their Three Dimensional Structure, *Space Sci. Rev.*, 89, 21–52, <https://doi.org/10.1023/A:1005291711900>, 1999.
- Gosling, J. T., Asbridge, J. R., Bame, S. J., and Feldman, W. C.: Solar wind speed variations: 1962–1974, *J. Geophys. Res.*, 81, 5061–5070, <https://doi.org/10.1029/JA081i028p05061>, 1976.
- Gosling, J. T., Asbridge, J. R., Bame, S. J., and Feldman, W. C.: Preferred solar wind emitting longitudes on the Sun, *J. Geophys. Res.*, 82, 2371–2376, <https://doi.org/10.1029/JA082i016p02371>, 1977.
- Guarnieri, F. L.: The Nature of Auroras During High-Intensity Long-Duration Continuous AE Activity (HILDCAA) Events: 1998 to 2001, in: *Recurrent Magnetic Storms: Corotating Solar Wind Streams*, edited by: Tsurutani, B., McPherron, R., Lu, G., Sobral, J. H. A., and Gopalswamy, N., American Geophysical Union, Washington, D.C., 235–243, <https://doi.org/10.1029/167GM19>, 2013.
- Hajra, R., Echer, E., Tsurutani, B. T., and González, W. D.: Solar cycle dependence of High-Intensity Long-Duration Continuous AE Activity (HILDCAA) events, relativistic electron predictors?, *J. Geophys. Res.-Space Phys.*, 118, 5626–5638, <https://doi.org/10.1002/jgra.50530>, 2013.
- Hajra, R., Echer, E., Tsurutani, B. T., and González, W. D.: Solar wind-magnetosphere energy coupling efficiency and partitioning: HILDCAAs and preceding CIR storms during solar cycle 23, *J. Geophys. Res.-Space Phys.*, 119, 2675–2690, <https://doi.org/10.1002/2013JA019646>, 2014a.
- Hajra, R., Echer, E., Tsurutani, B. T., and González, W. D.: Superposed epoch analyses of HILDCAAs and their interplanetary drivers: Solar cycle and seasonal dependences, *J. Atmos. Solar-Terr. Phys.*, 121, 24–31, <https://doi.org/10.1016/j.jastp.2014.09.012>, 2014b.
- Hapgood, M. A.: A double solar cycle in the 27-day recurrence of geomagnetic activity, *Ann. Geophys.*, 11, 248–253, 1993.
- Heber, B., Sanderson, T., and Zhang, M.: Corotating interaction regions, *Adv. Space Res.*, 23, 567–579, [https://doi.org/10.1016/S0273-1177\(99\)80013-1](https://doi.org/10.1016/S0273-1177(99)80013-1), 1999.
- Jian, L., Russell, C. T., Luhmann, J. G., and Skoug, R. M.: Properties of Stream Interactions at One AU During 1995–2004, *Sol. Phys.*, 239, 337, <https://doi.org/10.1007/s11207-006-0132-3>, 2006.
- Klausner, V., Papa, A., Mendes, O., Domingues, M., and Frick, P.: Characteristics of solar diurnal variations: A case study based on records from the ground magnetic station at Vassouras, Brazil, *J. Atmos. Solar-Terr. Phys.*, 92, 124–136, <https://doi.org/10.1016/j.jastp.2012.10.007>, 2013.
- Klausner, V., González, A. O., Domingues, M. O., Mendes, O., and Papa, A. R. R.: Study of local regularities in solar wind data and ground magnetograms, *J. Atmos. Solar-Terr. Phys.*, 112, 10–19, <https://doi.org/10.1016/j.jastp.2014.01.013>, 2014.
- Klausner, V., Domingues, M. O., Mendes, O., da Costa, A. M., Papa, A. R. R., and González, A. O.: Latitudinal and longitudinal behavior of the geomagnetic field during a disturbed period: A case study using wavelet techniques, *Adv. Space Res.*, 58, 2148–2163, <https://doi.org/10.1016/j.asr.2016.01.018>, 2016a.
- Klausner, V., Papa, A. R. R., Cândido, C. M. N., Domingues, M. O., and Mendes, O.: An alternative way to identify local geomagnetically quiet days: a case study using wavelet analysis, *Ann. Geophys.*, 34, 451–462, <https://doi.org/10.5194/angeo-34-451-2016>, 2016. b.
- Krieger, A. S., Timothy, A. F., and Roelof, E. C.: A coronal hole and its identification as the source of a high velocity solar wind stream, *Solar Phys.*, 29, 505–525, <https://doi.org/10.1007/BF00150828>, 1973.
- McComas, D. J., Bame, S. J., Barker, P., Feldman, W. C., Phillips, J. L., Riley, P., and Griffée, J. W.: Solar Wind Electron Proton Alpha Monitor (SWEPAM) for the Advanced Composition Explorer, *Space Sci. Rev.*, 86, 563–612, 1998.
- Ofman, L. and Davila, J. M.: Alfvén wave heating of coronal holes and the relation to the high-speed solar wind, *J. Geophys. Res.-Space Physics*, 100, 23413–23425, <https://doi.org/10.1029/95JA02222>, 1995.
- Ojeda-González, A., Mendes, O., Menconi, V. E., and Domingues, M. O.: Daubechies wavelet coefficients: a tool to study interplanetary magnetic field fluctuations, *Geofísica Internacional*, 53, 101–115, [https://doi.org/10.1016/S0016-7169\(14\)71494-1](https://doi.org/10.1016/S0016-7169(14)71494-1), 2014.
- Ojeda-González, A., Klausner, V., Mendes, O., Domingues, M. O., and Prestes, A.: Characterization of the Complex Ejecta Measured In Situ on 19–22 March 2001 by Six Different Methods, *Solar Phys.*, 292, 160, <https://doi.org/10.1007/s11207-017-1182-4>, 2017a.
- Ojeda-González, A., Mendes, O., Calzadilla, A., Domingues, M. O., Prestes, A., and Klausner, V.: An Alternative Method for Identifying Interplanetary Magnetic Cloud Regions, *The Astrophys. J.*, 837, 156, <https://doi.org/10.3847/1538-4357/aa6034>, 2017b.
- Prestes, A., Rigozo, N., Echer, E., and Vieira, L.: Spectral analysis of sunspot number and geomagnetic indices (1868–2001), *J. Atmos. Solar-Terr. Phys.*, 68, 182–190, <https://doi.org/10.1016/j.jastp.2005.10.010>, 2006.
- Prestes, A., Klausner, V., Ojeda-González, A., and Serra, S. L.: Statistical analysis of solar wind parameters and geomagnetic indices during HILDCAA/HILDCAA* occurrences between 1998 and 2007, *Adv. Space Res.*, 60, 1850–1865, <https://doi.org/10.1016/j.asr.2017.06.023>, 2017.
- Smith, C. W., L’Heureux, J., Ness, N. F., Acuña, M. H., Burlaga, L. F., and Scheifele, J.: The ACE Magnetic Fields Experiment, *Space Sci. Rev.*, 86, 613–632, <https://doi.org/10.1023/A:1005092216668>, 1998.
- Smith, E. J. and Wolfe, J. H.: Observations of interaction regions and corotating shocks between one and five AU: Pioneers 10 and 11, *Geophys. Res. Lett.*, 3, 137–140, <https://doi.org/10.1029/GL003i003p00137>, 1976.

- Souza, A., Echer, E., Bolzan, M. J. A., and Hajra, R.: A study on the main periodicities in interplanetary magnetic field Bz component and geomagnetic AE index during HILDCAA events using wavelet analysis, *J. Atmos. Solar-Terr. Phys.*, 149, 81–86, <https://doi.org/10.1016/j.jastp.2016.09.006>, 2016.
- Tsurutani, B. T. and González, W. D.: The cause of high-intensity long-duration continuous AE activity (HILDCAAs): Interplanetary Alfvén wave trains, *Planet. Space Sci.*, 35, 405–412, [https://doi.org/10.1016/0032-0633\(87\)90097-3](https://doi.org/10.1016/0032-0633(87)90097-3), 1987.
- Tsurutani, B. T. and Ho, C. M.: A review of discontinuities and Alfvén waves in interplanetary space: Ulysses results, *Rev. Geophys.*, 37, 517–541, <https://doi.org/10.1029/1999RG900010>, 1999.
- Tsurutani, B. T., Gould, T., Goldstein, B. E., González, W. D., and Sugiura, M.: Interplanetary Alfvén waves and auroral (substorm) activity: IMP 8, *J. Geophys. Res.-Space Phys.*, 95, 2241–2252, <https://doi.org/10.1029/JA095iA03p02241>, 1990.
- Tsurutani, B. T., González, W. D., González, A. L. C., Tang, F., Arballo, J. K., and Okada, M.: Interplanetary origin of geomagnetic activity in the declining phase of the solar cycle, *J. Geophys. Res.-Space Physics*, 100, 21717–21733, <https://doi.org/10.1029/95JA01476>, 1995.
- Tsurutani, B. T., González, W. D., Guarnieri, F., Kamide, Y., Zhou, X., and Arballo, J. K.: Are high-intensity long-duration continuous AE activity (HILDCAA) events substorm expansion events?, *J. Atmos. Solar-Terr. Phys.*, 66, 167–176, <https://doi.org/10.1016/j.jastp.2003.08.015>, 2004.
- Tsurutani, B. T., González, W. D., González, A. L. C., Guarnieri, F. L., Gopalswamy, N., Grande, M., Kamide, Y., Kasahara, Y., Lu, G., Mann, I., McPherron, R., Soraas, F., and Vasyliunas, V.: Corotating solar wind streams and recurrent geomagnetic activity: A review, *J. Geophys. Res.-Space Phys.*, 111, a07S01, <https://doi.org/10.1029/2005JA011273>, 2006.
- Tsurutani, B. T., Echer, E., Guarnieri, F. L., and González, W. D.: The properties of two solar wind high speed streams and related geomagnetic activity during the declining phase of solar cycle 23, *J. Atmos. Solar-Terr. Phys.*, 73, 164–177, <https://doi.org/10.1016/j.jastp.2010.04.003>, 2011.
- Webb, D.: Solar and geomagnetic disturbances during the declining phase of recent solar cycles, *Adv. Space Res.*, 16, 57–69, [https://doi.org/10.1016/0273-1177\(95\)00315-6](https://doi.org/10.1016/0273-1177(95)00315-6), 1995.
- Zirker, J. B.: Coronal holes and high-speed wind streams, *Rev. Geophys.*, 15, 257–269, <https://doi.org/10.1029/RG015i003p00257>, 1977.